The Solution Behavior of Hydrophobically Associating Zwitterionic Polymer in Salt Water

Hong Chen,[1] Zi-Min Wang,[1,2] Zhong-Bin Ye,[1,2] Li-Juan Han[1,2]

[1]State Key laboratory of Oil and Gas Reservoir Geology and Exploitation, Southwest Petroleum University, Chengdu, People's Republic of China
[2]Chemistry and Chemical Engineering of Southwest Petroleum University, Chengdu, People's Republic of China
Correspondence to: H. Chen (E-mail: chenh@swpu.edu.cn)

ABSTRACT: The acrylamide-based hydrophobically associating zwitterionic polymer was prepared, which was composed of dimethyl-dodecyl-allyl ammonium chloride as hydrophobic group and carboxyl betaine 2-(4-acrylamido-propyl-dimethyl ammonic)-sodium acetate as functional group. Hydrophobically associating polyacrylamide (HAPAM) was also prepared for comparative study. The behaviors of polymers in pure water and salt solutions were investigated by the means of apparent viscosity test, laser light scattering, atomic force microscope, and fluorescence experiments. The viscosities of polymer solution increased with the increasing of salt concentration, which indicated that the addition of salt resulted in significant antipolyelectrolyte effect in the zwitterionic polymer solution. The results of dynamic laser light scattering experiment also showed that the average hydrodynamic diameters of the zwitterionic polymer molecules increased with the increasing of salt concentration. The network structures had been observed by atomic force microscope and the addition of salt strengthened the formation of network structures. The results of fluorescence experiment showed that the addition of salt could enhance the association of hyrophobically zwitterionic polymer. © 2013 Wiley Periodicals, Inc. J. Appl. Polym. Sci. **2014**, *131*, 39707.

INTRODUCTION

Over the past two decades, hydrophobically associating polymers have attracted considerable attention because of their outstanding solution properties and numerous practical applications.[1–5] These polymers exhibit a strong tendency to self-associate via inter- or intrapolymeric interactions of the hydrophobic side chains, and have possible applications in food thickeners, coatings, paints, enhanced oil recovery, and water treatment, etc.[6–11] Even a very few of hydrophobic groups on polymer side chains can have a profound effect on their properties.[12–15] However, the viscosities of most hydrophobically associating polymers are sensitive to salt, which much confines its application in high salinity brine environment. Zwitterionic polymer is an important class of compound which contains cationic and anionic groups on the same molecule of polymer.[16–23] When the electrolyte is added to zwitterionic polymer aqueous solution, the physical attraction between the equivalent anions and cations are weakened and the zwitterionic polymer will stretch to a random coil conformation, so the viscosity of the polymer solution can increase with the addition of salt.[24] This is known as the antipolyelectrolyte effect.[25] At present, many betaine zwitterionic polymers have been reported, such as sulfo-,[26] carbo-,[27–29] and phospho- betaine

zwitterionic polymers.[30] They have been applied in bioseparations,[31] DNA assay,[32] and many other fields.[33–35] Copolymers containing acrylamide (AM) and zwitterionic monomer have a good resistance to high salt, but there are still some problems such as low molecular weight, low solution viscosity, etc.

Therefore, in order to improve the salt resistance of hydrophobically associating polymer and to improve solution viscosity of zwitterionic polymer, a kind of hydrophobically associating acrylamide-based betaine zwitterionic polymer was prepared, which was composed of acrylamide, dimethyl-dodecyl-allyl ammonium chloride (MDAC) as hydrophobic monomer, and 2-(4-acrylamido-propyl-dimethyl ammonic)-sodium acetate (AMPA) as functional monomer. Solution behavior of the terpolymer in salt water was special and a little different with those of zwitterionic copolymers because of introduction of hydrophobic monomer MDAC.

The chemical structure of polymer was showed in Figure 1.

EXPERIMENTAL

Materials
The carbo-betaine functional monomer was synthesized from *N,N*-dimethyl-propanediamine as raw material through two steps described in reference.[36] AM and hydrophobic monomer
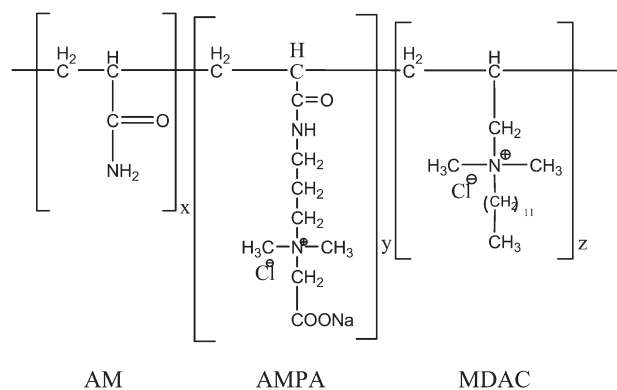
Figure 1. Chemical structure of zwitterionic polymer.

MDAC were purchased from Chengdu Kelong chemical company as analytical pure products.

Characterization of Monomer

The betaine monomer AMPA synthesized in this study was characterized by IR and ^{1}H-NMR. IR spectra were obtained by a Paragon 100 spectrometer (PE cooperation, USA) with AMPA samples embedded in KBr pellets in the experiment. ^{1}H-NMR spectra were obtained by an Avance spectrometer (Bruker Instruments, Switzerland). The sample was dissolved in D_2O and using TMS as an internal standard in the test of ^{1}H-NMR.

Synthesis of Polymers

The monomers of AM, AMPA, and MDAC were dissolved in water and purged with nitrogen for 1 h at 25°C. The reaction was initiated by the addition of sodium bisulfite and ammonium persulfate(mol ratio 1:1, total amount 0.04 wt %). Polymerization reactions were carried out at 50°C in a 250 mL thermo stated glass reactor equipped with magnetic stirrer and lasts at least 4 h. The polymers were precipitated in an ethanol/acetone mixture. The product was dried under vacuum drier for more than 2 days at 30°C. The polymer of hydrophobically associating polyacrylamide (HAPAM) without betaine comonomer for contratest study was also synthesized under identical conditions. The compositions of the polymers are listed in Table I.

Apparent Viscosity

Polymers were dissolved in pure water and brine waters. Solution viscosities of the polymers were measured by a DV-III Ultra programmable rheometer (Brookfield Instruments, USA) at 25°C. The 0# spindle was selected, and the rotation rate was 6 r min^{-1}, corresponding shear rate being 7.34 s^{-1}. The pH value of polymer solution was 7 in all the experiments in this article.

Table I. The Compositions of the Polymers

Sample	AM (%)	AMPA (%)	MDAC (%)
Z-Polymer	88.0	10.0	2.0
HAPAM	98.0	—	2.0

Laser Light Scattering

Laser light scattering measurements were performed with a Brookhaven instrument BI-200SM at a wavelength of 532 nm with the experimental temperature being 25°C. For light scattering experiments, solvent and polymer solutions were respectively filtered through 0.2 μm and 0.8 μm Millipore filter into the cylindrical scattering cells before the experiment. The average molecular weight of zwitterionic polymer was obtained by static laser light scattering.

When a laser light hits polymer particles which are small compared to the wavelength, the light scatters in all directions. For the static laser light scattering, the angular dependence of the excess absolute time-average scattered intensity, known as the Rayleigh ratio $R_{vv}(q)$, is related to the weight-average molecular mass (M_w), the second virial coefficient A_2, and the z-average root-mean-square radius of gyration $<R_g^2>_z^{1/2}$ (or $<R_g>$), as the polymer solution is dilute enough. For long polymer chains, the Berry plot is normally used as follows:

$$\left(\frac{KC}{R_{vv}(q)}\right)^{1/2} \approx \left(\frac{1}{M_W}\right)^{1/2}\left(1+\frac{1}{6}<R_g^2>q^2\right)(1+A_2M_wC) \quad (1)$$

where $K = 4\pi^2n^2 (dn/dC)^2/(N_A\lambda^4)$ and $q = (4\pi n/\lambda) \sin(\theta/2)$ with n, dn/dC N_A, and λ being the solvent refractive index, differential refractive index increment, Avogadro's number, and the wavelength of light in a vacuum, respectively.

Dynamic laser light scattering can be used to determine hydrodynamic radius $<R_h>$. In dynamic laser light scattering, the Laplace inversion of a measured intensity—intensity time correlation function $G^{(2)}(t,q)$ in the self-beating mode results in a line-width distribution $G(\Gamma)$. The distance between the particles in the solution is constantly changing with relaxation time τ, which is contained about the time scale of movement of the particles. Thus a time-dependent fluctuation in the scattering intensity can be gotten. The diffusion coefficient D can be derived at a single angle or at a range of angles depending on $1/\tau$.

$$\frac{1}{\tau} = Dq^2 \quad (2)$$

With the scattering vector q

$$q = \frac{4 \pi n}{\lambda}\sin\left(\frac{\theta}{2}\right) \quad (3)$$

$$\Gamma = Dq^2 \quad (4)$$

For a pure diffusive relaxation, $(\Gamma/q^2)_{q\to0, c\to0}$ is equal to the translational diffusion coefficient D, which is further related to the hydrodynamic radius R_h by the Stokes—Einstein equation:

$$R_h = \frac{kT}{6\pi\eta_0 D} \quad (5)$$

where k, T, and η_0 being the Boltzmann constant, the absolute temperature, and the solvent viscosity, respectively.

Atomic Force Microscope

The samples were imaged by using a Nanoscope IIIa (Digital Instruments, Santa Barbara, CA) to observe the

micromorphology of polymers in pure water and brine water. The preparation of samples was described elsewhere.[9]

Fluorescence Spectroscopy

The fluorescence spectra were obtained with a Cary Eclipse Fluorescence Spectrophotometer using pyrene as fluorescent probe in this study. Pyrene obtained from Aldrich Chemical Co. was recrystallized from absolute ethanol. The pyrene concentration in the experiment was 10^{-6} mol L^{-1} and the method of measurement can also be seen in our previous study. [9]

RESULTS AND DISCUSSION

Characterization

The monomer, carboxyl betaine 2-(4-acrylamido-propyl-dimethyl ammonic)-sodium acetate, synthesized in this article was characterized by IR, ^{1}H-NMR. The results were shown as follows: 1680 (m, C=C), C=C absorption peak, is medium and between 1600 and 1680. 1734 (s, C=O), C=O absorption peak, is strong and between 1580 and 1850. 1600 (CONHR), the absorption peak of N-H of acrylamide, is ~1600. 3575 (w, N-H), the peak of NH_2 or NH, is medium or weak between 3210 and 3590. 1398, 2950 (-CH_3), 1481 (-CH_2-), the peaks of alkyl C-H, is usually between 1340 and 1465, 2850 and 3000. 2950 (NR_4^+), the peak of NR_4^+, is between 2250 and 3200. 1123 (C-N), the peak of C-N, is usually between 1030 and 1230. It can be seen that C=C, C=O, and CONHR appear in the molecule, so acrylamide group exists. The NR_4^+ and C-N show that quaternary ammonium salt exists.

^{1}HNMR: δ 4.7 (D_2O), 3.293 (-CH_3), 1.860—2.860 (NH_2-CH_2-CH_2-CH_2-NHR_2), 2.823 (CONHR), 5.7 and 6.3 (-CH_2=CH-CONHR), 3.071 (-CH_2-COO^-).

The groups of target molecule are reflected in ^{1}HNMR.

The zwitterionic polymer synthesized in this article was also characterized by ^{1}H-NMR. The result was shown as follows:

^{1}HNMR: δ 4.7 (D_2O), 3.149 (-CH_3), 1.737-3.037 (NH_2-CH_2-CH_2-CH_2-NHR_2), 5.701 and 6.239 (CH_2-CH_2-CONHR), 3.149 (-CH_2-COO^-).

Viscosity Behavior

Most zwitterionic polymers, especially polysulfobetaines, are generally slightly soluble in pure water. While, the addition of low molecular weight electrolytes such as NaCl is favorable to the solubilization of the polymer, so these polybetaines tend to be dissolved in salt water than in pure water. The zwitterionic polymer synthesized in this article can be dissolved in pure water, although it took a longer time to be dissolved than other water soluble polymer did, such as HPAM or HAPAM. The viscosities of zwitterionic polymer in pure water and salt water were measured and the results are shown in Figure 2.

From Figure 2, it can be seen that the viscosities of zwitterionic polymer increase with the increasing of polymer concentration in both pure water and salt solutions. When the concentration of polymer is constant, the viscosity of the solution increases with the increasing of salt. This phenomenon becomes more obvious when salt concentration is higher than 3 wt %. The addition of salt is favorable for the expansion of the molecular
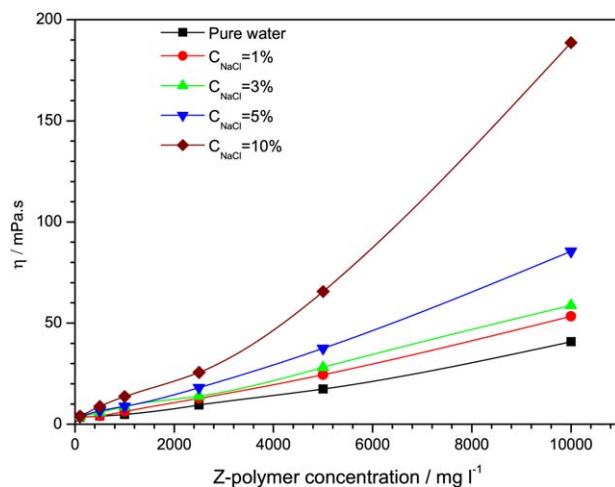

Figure 2. Viscosity as a function of polymer concentration. [Color figure can be viewed in the online issue, which is available at wileyonlinelibrary.com.]

side chains because of antipolyelectrolyte effect and the solution viscosity increases correspondingly.

The effect of the addition of salt on the viscosity of Z-polymer and HAPAM was investigated, with the concentrations of both polymer solutions being 2500 mg L^{-1} in the experiment, and the results are shown in Figure 3. From Figure 3, it can be seen that the viscosity of zwitterionic polymer increases with the increasing of salt concentration, while the viscosity of HAPAM decreases sharply in the presence of salt. The introduction of betaine monomer makes the polymer coil expand in brine water, which favors the intermolecular association of hydrophobic groups, so that the polymer shows a remarkable salt thickening ability, especially in high brine waters. The phenomenon shows that the salt resistance of hydrophobically associating polymer is considerably enhanced by the introduction of the betaine monomer.
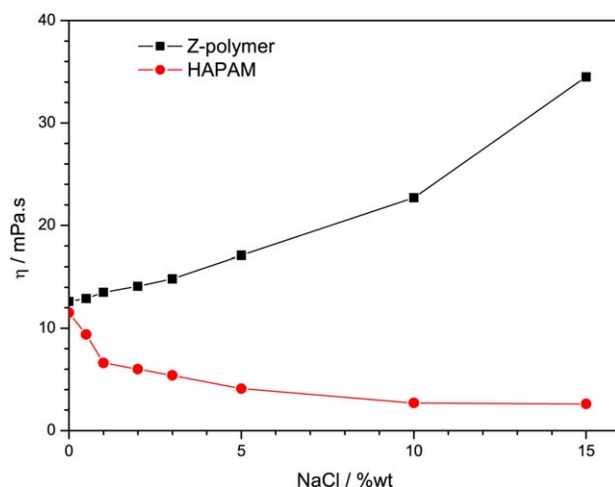
Figure 3. Variation of viscosities of polymer solutions with the increasing of salt concentration (C_p = 2500 mg L^{-1}). [Color figure can be viewed in the online issue, which is available at wileyonlinelibrary.com.]
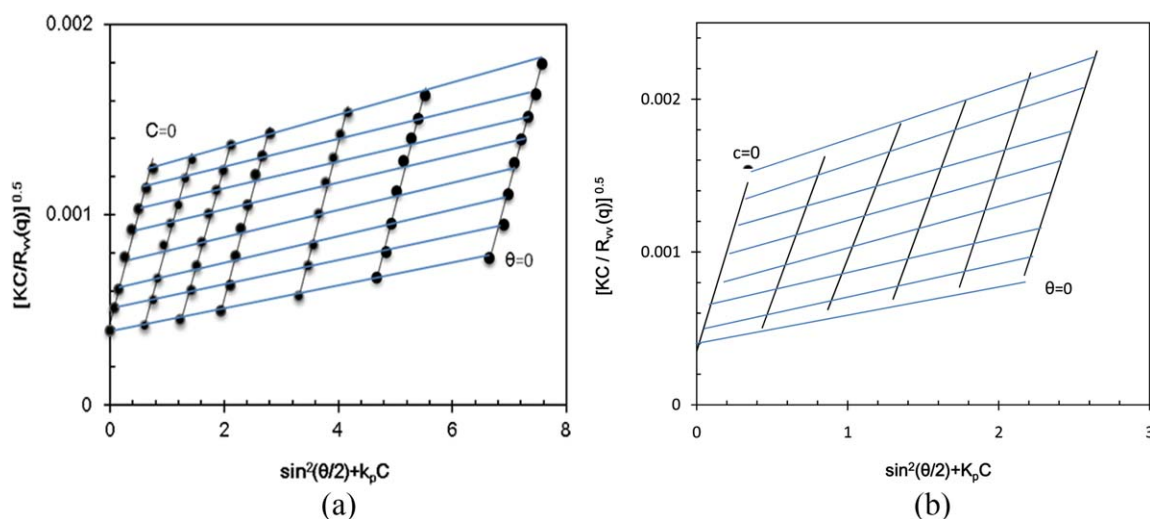
Figure 4. The Berry plot of Zwitterionic polymer and HAPAM in pure water. (a) Zwitterionic polymer, (b) HAPAM. [Color figure can be viewed in the online issue, which is available at wileyonlinelibrary.com.]

Static Laser Light Scattering

If the left hand side of eq. (1) is plotted against $\sin^2(\theta/2) + k_p C$, where k_p is an arbitrary plotting constant chosen purely for convenience in viewing the results, a grid-like plot is obtained. Two sets of, typically, parallel lines make up the grid. One set consists of angular measurements at each concentration, and one set consists of concentration measurements at each angle. Extrapolating the angular measurements to zero angle for each concentration yields a straight line in c. The slope of this line yields A_2. Extrapolating the concentration measurements to zero concentration for each angle yields a straight line in $\sin^2(\theta/2)$. The slope divided by the intercept of this line yields the $<R_g>$. The intercept of both extrapolated lines (the double extrapolation to zero angle and zero concentration) yields M_w, the weight-average molecular mass of polymer. M_w is the most important parameter of a polymer. Static light scattering offers an absolute method for its measurement.

The grid-like plot is showed in Figure 4(a,b), and the the M_w, A_2, and $<R_g>$ are illustrated in Table II.

From Table II we can see that the weight-average molecular mass of both polymers is very close, however, there are big differences in the A_2 and $<R_g>$ of these polymers. The zwitterionic polymer coils tend to shrink in pure water because of the inner salt effect, and the intramolecular association of hydrophobic groups bonded on the zwitterionic polymer backbone makes the coils shrink closely, which leads to the $<R_g>$ of zwitterionic polymer far smaller than that of HAPAM. The greater A_2 means that HAPAM has a better solubility than that of zwitterionic polymer.

Table II. The Parameters of Polymers

| Polymer	M_w (g mol^{-1})	A_2 (cm^3 mol g^{-2})	$<R_g>$ (nm)
Z-Polymer	5.21×10^6	1.74×10^{-6}	127.4
HAPAM	6.17×10^6	4.58×10^{-4}	223.5

Dynamic Laser Light Scattering

Since the 60s of the twentieth century, dynamic laser light scattering technique had become the main means of sub micron, nanometer particle size measurement. There are many algorithm, such as cumulant method, exponential sampling method, NNLS, and CONTIN algorithm.[37] Among them the CONTIN algorithm is always used for data processing and is ideal for heterodisperse or polydisperse systems that cannot be resolved with the cumulant method. The polymer concentration is constant at 100 mg L^{-1} and the results are shown in Figure 5.

The average diameters ($<R_h>$) of zwitterionic polymer are much smaller than those of HAPM in pure water or low salinity water, though the weight-average molecular masses (M_w) of these two polymers are very close. The average diameter $<R_h>$ of zwitterionic polymer increases steadily with the increasing of salt concentration, however, $<R_h>$ of HAPAM decreases due to the addition of salt. The reason is that the zwitterionic polymer
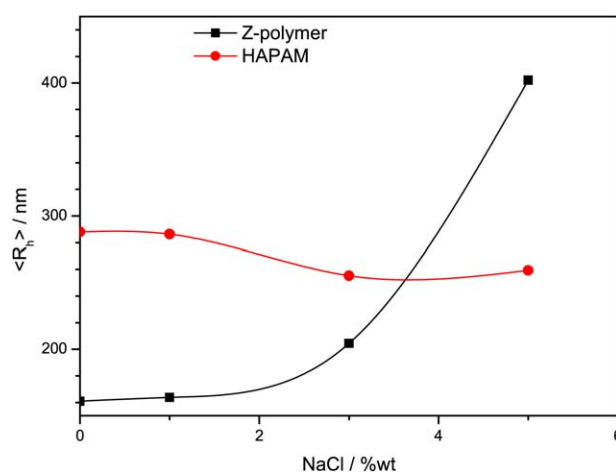
Figure 5. The $<R_h>$ of polymers as a function of salt. [Color figure can be viewed in the online issue, which is available at wileyonlinelibrary.com.]
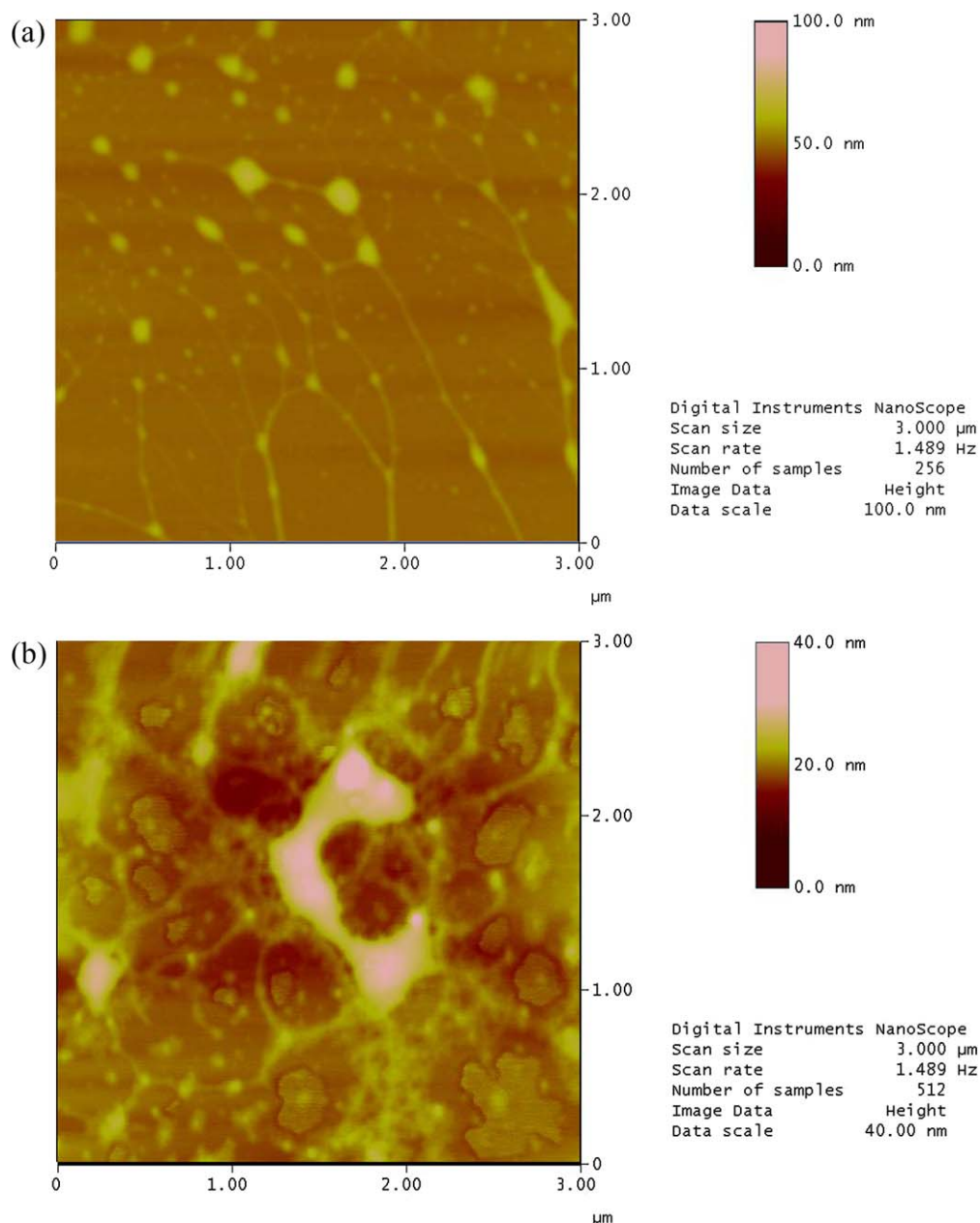
Figure 6. AFM of zwitterionic polymer (concentration 500 mg L^{-1}). (a) In pure water, (b) In 3 wt % salt water. [Color figure can be viewed in the online issue, which is available at wileyonlinelibrary.com.]

coils shrink closely in pure water or low salinity water because of the inner salt effect and the intramolecular association, so the $<R_h>$ of zwitterionic polymer is smaller than that of HAPAM. When the salt was higher, the zwitterionic polymer molecules could expand by charge repulsion as a result of the inner salt bond being opened, and the intermolecular association of hydrophobic groups could lead to the size increase of aggregates formed by zwitterionic polymer, which could certainly increase the $<R_h>$ of zwitterionic polymer. This phenomenon could well explain the salt thickening behavior of zwitterionic polymer solution. However, the addition of salt could make the HAPAM polymer coils shrink, and the diame-

ters of polymer (without betaine groups) aggregates decrease smoothly during the process of the addition salt. The results show that the hydropobically associating polymers exhibits an excellent anti-salinity property as the betaine monomer was introduced into the macromolecular chains.

Atomic Force Microscope

Atomic force microscope (AFM) is used to observe structures of polymer solution on mica. In this article, the polymer solution was deposited on freshly cleaved natural mica and dried by nitrogen. The microstructure morphologies of zwitterionic

polymer in salt water and pure water had been performed and the results are shown in Figure 6.

From Figure 6(a), it can be seen that distinct globular structure with a few local network formed when the zwitterionic polymer concentration is 500 mg L^{-1} in pure water. It is well known that network structures can be formed when the polymer concentration exceeds its critical overlap concentration. Because the concentration is not high enough and the attraction of zwitterion makes the zwitterionic polymer shrink to a coil conformation, the whole network cannot be formed, only a few local network and globular aggregates.

Figure 6(b) shows that the globular aggregates are stretched with the addition of salt at the same polymer concentration 500 mg L^{-1}. The addition of NaCl causes macromolecules to spread and adopt a random coil conformation because of antipolyelectrolyte effect, which could enhance the viscosity of zwitterionic polymer solution. The reason is that intramolecular force is weakened and intermolecular force is strengthened when salt is added.

Fluorescence Spectrum Experiment

Pyrene is a strongly hydrophobic polyaromatic hydrocarbon with very low solubility in water. Amphiphilic polymers spontaneously form micelles and then the small hydrophobic domains present in such solutions are capable of solubilization of pyrene. It is well known that each fluorescence spectrum of pyrene monomer has one to five vibronic peaks from shorter to longer wavelength. Steady-state fluorescence spectra for pyrene solubilized in various zwitterionic polymer or HAPAM concentration solutions of pure water and salt water were investigated. In salt water, the sodium chloride concentration was 3 wt %. A well-resolved pyrene monomer emission intensity (I_m) was at 373 nm. In addition to the "monomer" emission spectra, one also observes a broad peak excimer emission (I_e) at higher wavelength centered about at 475 nm corresponding to the excimer formation due to pyrene molecules in close vicinity. Excimer formation requires that an excited pyrene (P_y^*) and a pyrene in its ground state come into close proximity within the Py* lifetime. The results of fluorescence absorption intensity (I_e) as a function of zwitterionic polymer concentration in pure and brine water are showed in Figure 7.

From Figure 7, it can be seen that the values of I_e undergo a maximum with the increasing of polymer concentration. The value of I_e increases with the increasing of the polymer concentration when the concentration is lower than 3000 mg L^{-1} in brine water and 5000 mg L^{-1} in pure water, respectively. However, when the concentration is higher, the value of I_e decreases with the increasing of the polymer concentration. The reason is that hydrophobically zwitterionic polymer can form aggregates by self-assembly, and salt can strengthen the self-assembly behavior. With the increase of polymer concentration, more and more hydrophobic microdomains (or micelle) form. When the pyrene concentration is constant, the local concentration of the pyrene in hydrophobic microdomain undergoes a maximum with the increase of the polymer concentration, directly corresponding to the variation of I_e.

The ratio of the peaks 384 nm (I_3) and 373 nm (I_1) in the absorption spectra is strongly dependent on the polarity of microenvironment for pyrene. The I_3/I_1 ratio in the fluorescence spectrum of
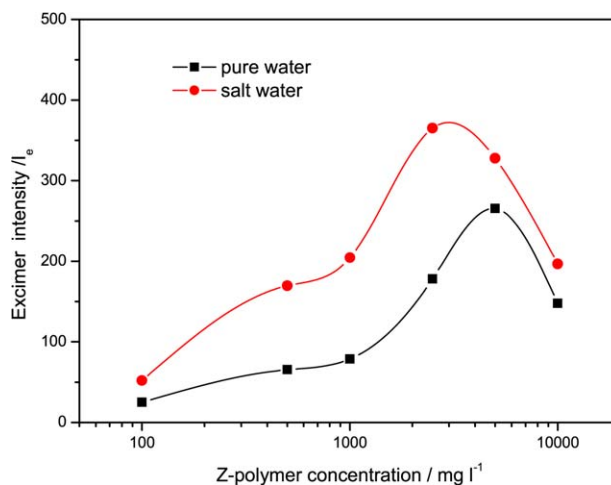
Figure 7. The I_e as a function of polymer concentration. [Color figure can be viewed in the online issue, which is available at wileyonlinelibrary.com.]

pyrene is measured in zwitterionic polymer solutions with or without salt, and the results are shown in Figure 8.

From Figure 8, it can be seen that the I_3/I_1 ratio is about 0.70 in salt solution and 0.65 in pure water at low concentration (100 mg L^{-1}), which is higher than in free polymer water (~0.58). It indicates that there exist a few hydrophobic aggregates in this concentration range even if the concentrations of the polymers are very low, and the polarity of the system is strengthened with the addition of salt. When the polymer concentration is higher than 640 mg L^{-1} in salt water and 1330 mg L^{-1} in pure water, the I_3/I_1 ratios start to increase significantly. With the increase of polymer concentration, more and more hydrophobic microdomains (or micelles) have been formed by hydrophobic interaction and a large number of pyrenes are dissolved into the hydrophobic microdomains (or micelles). When the polymer concentration reached 5000 mg L^{-1} in salt water or 6500 mg L^{-1} in pure water, there is a turning point. After this turning point, the value of I_3/I_1 has a little change with the increasing of polymer
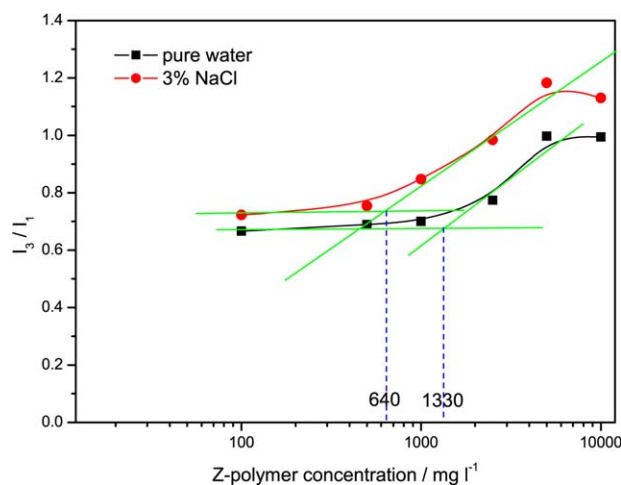
Figure 8. The ratio of I_3/I_1 as a function of polymer concentration. [Color figure can be viewed in the online issue, which is available at wileyonlinelibrary.com.]

concentration. The results show that the salt can strengthen the association of hyrophobically zwitterionic polymer, which can also explain the salt thickening behavior of this polymer.

CONCLUSIONS

In this article, a kind of hydrophobically associating zwitterionic polymer was synthesized, and the properties were investigated in pure water and brine water. The viscosity of zwitterionic polymer rises with addition of salt, when the betaine monomer has been introduced into the polymer chains. Local network structure has formed when the zwitterionic polymer concentration is 500 mg L^{-1} in the AFM micrographs. The globular aggregates are stretched when salt is added and hydrodynamic radius $<R_h>$ of zwitterionic polymer increase steadily with the increasing of NaCl. Zwitterionic polymer shows remarkable salt thickening behavior and anti-salinity properties by the introduction of the betaine monomer. The results of fluorescence experiment show that the addition of salt can facilitate the aggregation of zwitterionic polymer solution. This polymer has a great prospect in petroleum development, especially in very high salinity oil reservoirs. In the future researches, the properties of thickening, resistance to high temperature and solubility should be improved, which could make the polymer be applied in chemical flooding of high temperature and high salinity reservoir as soon as possible.

ACKNOWLEDGMENTS

REFERENCES

1. Zhong, C.; Huang, R.; Ye, L.; Dai, H. J. *Appl. Polym. Sci.* **2006**, *101*, 3996.

2. Han, L.; Ye, Z.; Chen, H.; Luo, P. *Acta Phys.: Chim. Sin.* **2012**, *28*, 1405.

3. Chen, H.; Li, E. X.; Ye, Z. B.; Han, L. J.; Luo, P. Y. *Acta Phys.: Chim. Sin.* **2011**, *27*, 671.

4. Ma, J.; Huang, R.; Zhao, L.; Zhang, X. J. *Appl. Polym. Sci.* **2005**, *97*, 316.

5. Winnik, F. M.; Regismond, S. T. A.; Goddard, E. D. *Langmuir* **1997**, *13*, 111.

6. Dragan, S.; Ghimici, L. *Polymer* **2001**, *42*, 2886.

7. Seigou, K.; Mohd, M.; Kouji, K.; Haruki, M.; Iriany, K.; Norbert H.; Manfred, S. *Polym. J.* **2002**, *34*, 253.

8. Zhong, C.; Ye, Z.; Luo, P.; Chen, H. *Polym. Bull.* **2009**, *62*, 79.

9. Chen, H.; Ye, Z.; Han, L.; Luo, P. J. *Appl. Polym. Sci.* **2012**, *123*, 2397.

10. Gouveia, L. M.; Grassl, B.; Müller, A. J. *J. Colloid Interface Sci* **2009**, *333*, 152

11. Umar, Y.; Abu-Sharkh, B. F.; Ali, S. A. J. *Appl. Polym. Sci.* **2005**, *98*, 1404

12. Hussein, I. A.; Asrof Ali, S. K.; Suleiman, M. A.; Umar, Y. *Euro. Polym. J.* **2010**, *46*, 1063.

13. Maia, A. M. S.; Borsali, R.; Balaban, R. C. *Mater. Sci. Eng.: C* **2009**, *29*, 505

14. Zhao, Y.; Zhou, J.; Xu, X.; Liu, W.; Zhang, J.; Fan M.; Wang, J. *Colloid Polym. Sci.* **2009**, *287*, 237.

15. Kathmann, E. E.; White, L. A.; McCormick, C. L. *Polymer* **1997**, *38*, 879.

16. Jiang, G.; Huang, L.; Li, B.; Lv, C.; Li, R.; Liu, F. *J. Appl. Polym. Sci.* **2012**, *123*, 66.

17. Bonte, N.; Laschewsky, A.; Mayer, B.; Vermylen, V. *Macromol. Symp.* **1996**, *102*, 273.

18. Johnson, K. M.; Fevola, M. J.; McCormick, C. L. J. *Appl. Polym. Sci.* **2004**, *92*, 647.

19. Miyazawa, K.; Winnik, F. M. *Macromolecules* **2002**, *35*, 2440.

20. Miyazawa, K.; Winnik, F. M. *Macromolecules* **2002**, *35*, 9536.

21. Miyazawa, K.; Winnik, F. M. J. *Phys. Chem. B* **2003**, *107*, 10677.

22. Grassl, B.; Mathis, A.; Rawiso, M.; Galin, J. C. *Macromolecules* **1997**, *30* 2075.

23. Rodriguez, M.; Xue, J.; Gouveia, L.M.; Muller, A. J.; Saez, A. E.; Rigolini, J.; Grassl, B. *Colliod Surf. A: Physicochem. Eng. Aspects* **2011**, *373*, 66.

24. Fevola, M. J.; Bridges, J. K.; Kellum, M. G.; Hester, R. D.; McCormick, C. L. J. *Appl. Polym. Sci.* **2004**, *94*, 24.

25. Georgiev, G. S.; Kamenska, E. B.; Vassileva, E. D.; Kamenova, I. P.; Georgieva, V. T.; Iliev, S. B.; Ivanov, I. A. *Biomacromolecules* **2006**, *7*, 1329.

26. Chang, Y.; Liao, S.-C.; Higuchi, A.; Ruaan, R.-C.; Chu C.-W. Chen, W.-Y. *Langmuir* **2008**, *24*, 5453.

27. Al-Muallem, H. A. J. *Appl. Polym. Sci.* **2011**, *119*, 1477.

28. Gui, Z.; Du, B.; Qian, J.; An, Q.; Zhao, Q. J. *Colloid Interface Sci.* **2011**, *353*, 98.

29. Lezov, A. V.; Vlasov, P. S.; Lezov, A. A.; Domnina N. S.; Polushina, G. E. *Polym. Sci. Ser. A* **2011**, *53*, 1012.

30. Ali, S. A.; Abu-Thabit, N. Y.; Al-Muallem, H. A. J. *Polym. Sci. Part A* **2010**, *48*, 5693.

31. Kudaibergenov, S. E.; Didukh, A. G.; Zhumadilova, G. T.; Koizhaiganova, R. B.; Bimendina, L. A.; Jung-Gyun, N.; Geckeler, K. E. *Macromol. Symp.* **2004**, *207*, 153.

32. Sitnikova, T. A.; Rakhnyanskaya, A. A.; Yaroslavova, E. G.; Sergeev-Cherenkov, A. N.; Khomutov, G. B.; Grinberg, V. Ya.; Burova, T. V.; Yaroslavov, A. A.. *Polym. Sci. Ser. A* **2009**, *51*, 630.

33. González Coronel, V. J. Jiménez-Regalado, E. J. *Polym. Bull.* **2011**, *67*, 251.

34. Doyaguez, Elisa, G.; Parra, F.; Corrales, G.; Mayoralas, A. F.; Gallardo, A. *Polymer* **2009**, *50*, 4438.

35. Johnson, K. M.; Fevola, M. J.; McCormick, C. L. J. *Appl. Polym. Sci.* **2004**, *92*, 647.

36. Lowe, A. B.; McCormick, C. L. *Chem. Rev.* **2002**, *102*, 4177.

37. Yu, L.; Yang, G.; He, Z.; Li, Y. *Opto-Electronic Eng.* **2006**, *33*, 64.